ELSEVIER

Journal of Photochemistry and Photobiology A: Chemistry 91 (1995) 145–152

Journal of PHOTOCHEMISTRY AND PHOTOBIOLOGY A:CHEMISTRY

Photodegradation of surfactants XIV. Formation of NH_4^+ and NO_3^- ions for the photocatalyzed mineralization of nitrogen-containing cationic, non-ionic and amphoteric surfactants

Hisao Hidaka [a,*], Kayo Nohara [a], Jincai Zhao [a], Ezio Pelizzetti [b], Nick Serpone [c]

[a] *Department of Chemistry, Meisei University, 2-1-1, Hodokubo, Hino, Tokyo 191, Japan*

[b] *Dipartimento di Chimica Analitica, Universita di Torino, Via Pietro Giuria 5, 10125 Torino, Italy*

[c] *Department of Chemistry, Concordia University, 1455, de Maisonneuve Blvd. West, Montréal, Que. H3G1M8, Canada*

Received 16 November 1994; accepted 10 March 1995

Abstract

The photo-oxidation of cationic, non-ionic and amphoteric nitrogen-containing surfactants (*N*-dodecylpyridinium chloride (DPC) and benzyl-tetradecyldimethyl-ammonium chloride (BTDAC); dodecanoyl-*N*-(2-hydroxyethyl) amide (N-DHA) and dodecanoyl-*N*,*N*-bis(2-hydroxyethyl) amide (N,N-DHA); dodecyl-β-alanine (C_{12}-β-Ala) and *N*-(2-hydroxydodecyl)-*N*-(2-hydroxyethyl)- β-alanine (C_{12}-β-HAA)) was examined in UV-illuminated, air-equilibrated aqueous titania suspensions. Variations in the surface tension of the photo-oxidized surfactant solutions were monitored as a function of the irradiation time. The formation of ammonium and nitrate ions, together with the evolution of carbon dioxide, was investigated for the various surfactant chemical structures to obtain mechanistic information on the mineralization pathways. The yield of NH_4^+ ions was 4–13 times greater than the yield of NO_3^- ions. The amount of NH_4^+ ions formed depends on the structures of the surfactants. Mechanistic details of the photocleavage of the alkyl chains were inferred by probing the oxidation of sodium dodecanoate. The intermediates formed during the temporal photomineralization of the surfactant species were identified by high-frequency Fourier transform (FT) proton nuclear magnetic resonance (NMR) spectroscopy.

Keywords: Surfactant; Photodegradation; Photo-oxidation; Titanium dioxide; Photocatalyst

1. Introduction

Various domestic and industrial surfactants are disposed of in rivers and lakes without prior treatment. An amount of surfactant in excess of the permissible biodegradation range places severe stress on the aquatic ecosystem. Finding new treatments or remedial techniques is an important task from the viewpoint of environmental conservation. Five procedures have been considered as potentially applicable in the short term for the mineralization of surfactants in particular and organic pollutants in general; (1) bacterial biodegradation [1]; (2) synthesis of destructible surfactants [2]; (3) sonolysis [3]; (4) photolysis [4]; (5) photocatalytic degradation [5]. Each of these procedures has certain desirable characteristics and certain disadvantages from a practical viewpoint. Not all organic pollutants can be decomposed by bacterial biodegradation processes using activated sludge. Relatively long periods of time are usually required for complete decomposition. Utilization of molecularly designed destructible surfactants has been considered recently. However, these destructible surfactants have not been produced on an industrial scale because of the cost involved. Many studies have been performed on the photochemical degradation by hydroxyl radicals in the so-called "Advanced Oxidation Technologies", e.g. O_3/UV, H_2O_2/UV [4,6] and TiO_2/UV [7]. Of interest here is photo-oxidation using a TiO_2 (anatase) photocatalyst which has a band gap of 3.2 eV and provides several advantages.

We have focused much attention on the photocatalytic oxidation of surfactants. The hydrocarbon moiety in a surfactant is oxidized to CO_2 and H_2O. For anionic surfactants, the aromatic ring, which is difficult to biodegrade, is photo-oxidized more rapidly owing to facile attack by the active oxygen species generated on the TiO_2 photocatalyst surface on UV exposure [8]. Water-soluble sulfonate (or sulfate) and phosphonate groups are transformed into SO_4^{2-} and

* Corresponding author.

SSDI 1010-6030(95)04072-2

$H_2PO_4^-$ ions respectively [9]. By contrast, a cationic surfactant containing quaternary nitrogen is electrostatically repelled by the positively charged TiO_2 surface; this leads to a slow rate of mineralization. The pH value (pH 5.8) of the starting benzyl-tetradecyldimethyl-ammonium chloride (BTDAC) or *N*-dodecylpyridinium chloride (DPC) solution becomes more acidic (pH 4.5) because of the formation of a proton. The nitrogen moieties in BTDAC and DPC are converted to NH_4^+ and NO_3^- ions concomitantly. An earlier study showed that the quantity of ammonium formed is larger than that of nitrate ions [10]. A primary amine moiety in an organic compound is converted to an NH_4^+ ion, whereas a nitro group is converted to NO_3^- as pointed out by Matthews and coworkers [11]. In an *N*-heterocyclic structure, the nitrogen atom is transformed into both NH_4^+ and NO_3^- species [12]. The mechanisms underlying some of these observations have not yet been fully elucidated. Herein, we examine and compare the formation yields of ammonium ions and nitrate ions for various nitrogen-containing cationic, nonionic and amphoteric surfactants during their mineralization with an illuminated TiO_2 system. A mechanism for the mineralization of these surfactants is inferred on the basis of the photodegradation of both the hydrophobic alkyl chain and the hydrophilic ionic nitrogen moiety with the aid of the mineralization of a dodecanoate chain.

2. Experimental section

2.1. Chemicals and reagents

The cationic *N*-dodecylpyridinium chloride (DPC) and *N*-hexadecylpyridinium chloride were supplied by Wako Pure Chem. Ind. *N*-Butylpyridinium bromide was synthesized by reacting pyridine with butyl bromide and was recrystallized three times from acetone. The purity of the material was confirmed by IR and nuclear magnetic resonance (NMR) spectroscopies. Both ethylpyridinium bromide and benzyl-tetradecyldimethylammonium chloride (BTDAC) ($[CH_3(CH_2)_{11}\text{-}N^+(CH_3)_2CH_2C_6H_5]Cl^-$) were supplied by Tokyo Kasei Co. Ltd. and were employed without further purification. Dodecanoyl-*N*-(2-hydroxyethyl) amide (N-DHA) ($C_{11}H_{23}CONHCH_2CH_2OH$) and dodecanoyl-*N*,*N*-bis(2-hydroxyethyl) amide (N,N-DHA) ($C_{11}H_{23}CON(CH_2CH_2OH)_2$) were supplied by Toho Chem. Ind. Co. Ltd. The amphoteric surfactant *N*-(2-hydroxydodecyl)-*N*-(2-hydroxyethyl)-β-alanine (C_{12}-β-HAA) ($C_{10}H_{21}CH(OH)CH_2N(CH_2CH_2OH)CH_2CH_2\text{-}COONa$) was provided by Miyoshi Oil & Fat Co. Ltd; dodecyl-β-alanine (C_{12}-β-Ala) ($C_{12}H_{25}NHCH_2CH_2COONa$) was supplied by Lion Co. Ltd. The titanium dioxide employed was a generous gift by Degussa AG (approximately 80% anatase and 20% rutile form; Brunauer–Emmett–Teller (BET) surface area, approximately 55 $m^2\ g^{-1}$; particle size, about 30 nm; approximately 99.5% TiO_2 P-25, <0.3% Al_2O_3, <0.3% HCl, <0.2% SiO_2 and <0.01% Fe_2O_3) [13]. Deionized and distilled water was used throughout, unless otherwise noted.

2.2. Photodegradation procedures and analytical methods

A dispersion consisting of a surfactant solution (0.1 or 1 mM; volume, 50 ml) and TiO_2 (100 mg) was contained in a 70 ml Pyrex glass vessel and illuminated with a mercury lamp at wavelengths greater than 330 nm (Toshiba SHLS-1002A; 100 W) with continuous magnetic agitation. In all measurements, TiO_2 particles were removed by centrifugation followed by filtration through a Millipore membrane (0.22 μm). The surface tension was measured at ambient temperature with a De Nouy tensiometer, using a platinum ring of 1 cm in diameter, for a photodegraded aqueous solution (about 3 ml) after an appropriate irradiation time. The temporal evolution of CO_2 during photo-oxidation was assayed by gas chromatography (thermal conductivity detection) using a Porapack Q column. The proton NMR spectral profiles of surfactant/D_2O solutions (1 or 10 mM; volume, 10 ml), after various illumination times in the presence of TiO_2 particulates (20 mg), were monitored with a JEOL 500 MHz Fourier transform (FT) proton NMR spectrometer. The formation of NH_4^+ ions was followed with a JASCO ion chromatograph equipped with a Y-521 cationic column and a CD-5 conductivity detector; the eluent was nitric acid solution (4 mM). The evolution of NO_3^- ions was also monitored with a JEOL ion chromatograph using an I-524 anionic column; the eluent was a mixed solution (adjusted to pH 4) of phthalic acid (2.5 mM) and tris-(hydroxymethyl)-aminomethane (2.3 mM).

3. Results and discussion

The photocatalyzed mineralization of the surfactants reported here in particular and any organic substrate in general has its origin in the surface-trapped charge carriers (electrons: e_t^- or Ti^{3+}; holes: $^{\cdot}OH$ radicals [14] or equivalent oxygen species) generated following illumination of the photocatalyst TiO_2 with light energy greater than or equal to the band gap energy of 3.2 eV for the anatase form. These redox equivalents are positioned at the surface of the photocatalyst ready to initiate reduction and oxidation events [15]. To compete with the rapid recombination of charge carriers, even when trapped on the TiO_2 surface, the redox reactions require that the organic substrates (here the surfactants) are pre-adsorbed to some extent on the TiO_2 particle surface. The temporal course of the photo-oxidation follows the attack of the substrate by the $^{\cdot}OH$ radicals (or equivalent active oxygen species) to give, in some instances, $^{\cdot}OH$ radical adducts of the surfactants and/or H-atom abstraction of alkyl chains yielding hydrocarbon residue-centred radicals.

Past experience has shown that, in the photomineralization of surfactant substrates, three principal occurrences are worth noting: (1) suppression of foaming power; (2) oxidation of

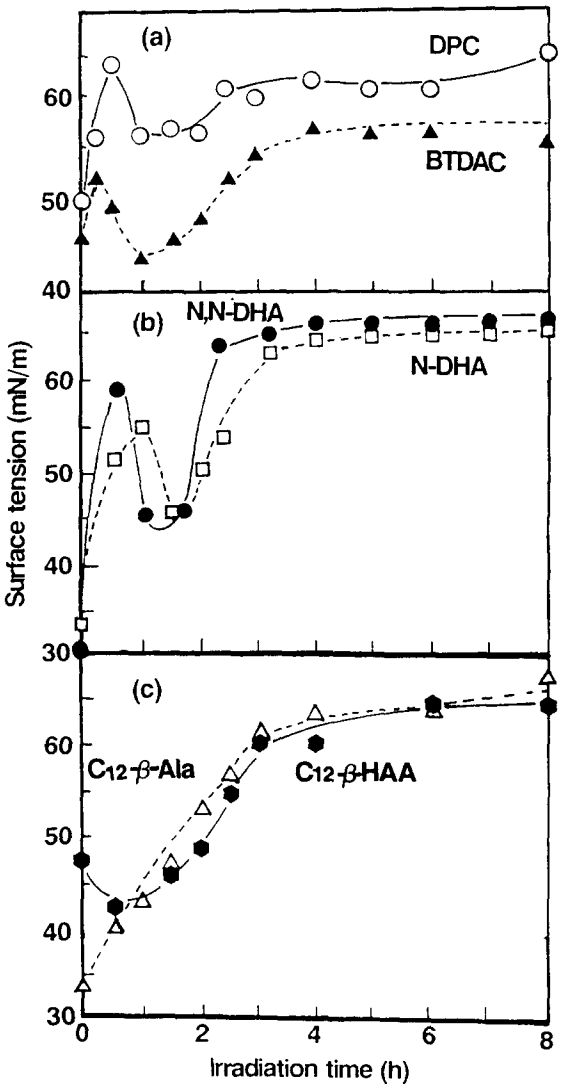

Fig. 1. Temporal behaviour of surface tension during the photo-oxidative degradation of (a) cationic surfactants: ○, DPC; ▲, BTDAC; (b) non-ionic surfactants: □, N-DHA; ●, N,N-DHA; (c) amphoteric surfactants: △, C_{12}-β-Ala; ●, C_{12}-β-HAA. Concentration, 1 mM.

the aromatic moiety (if any); (3) subsequent slower oxidation of the alkyl chain residues [16]. The surfactants containing S and P atoms are oxidized to form SO_4^{2-} and $H_2PO_4^-$, whereas N-containing surfactants form NO_3^- and NH_4^+ ions.

3.1. Photocatalysed oxidation

The relationship between the surface tension and the irradiation time for the three classes of cationic (DPC, BTDAC), non-ionic (N-DHA and N,N-DHA) and amphoteric (C_{12}-β-HAA and C_{12}-β-Ala) surfactants is examined in Figs. 1(a)–1(c). The surface tension of the photodegraded cationic and non-ionic surfactants increases rapidly during the first hour of irradiation. Further illumination leads first to a decrease in surface tension and subsequently to a continual increase up to about 70 mN m^{-1}. For the amphoteric surfactant C_{12}-β-HAA, the surface tension decreases slightly during the first hour and then increases gradually with further irradiation. No such decrease is noted in the case of C_{12}-β-Ala solutions, the surface tension increasing continually with irradiation time from an initial value of about 33 mN m^{-1} (see Fig. 1(c)). Since the surface activities of the photodegraded solution become poorer (approach the surface tension of water) with irradiation (approximately 3 h), the surfactant molecules in the solutions must be destroyed by that time. Initially, the hydroxyethyl group in the N-DHA and N,N-DHA structures or the pyridinium ring in DPC, which are hydrophilic, are ruptured to give relatively poor surface-active intermediates. Subsequently, parts of the hydrophobic alkyl chain in these intermediates are aligned at the solution/air interface causing a temporary decrease in surface tension. The decrease for C_{12}-β-HAA implies the formation of mixed micelles consisting of the starting surfactant and the photo- oxidized intermediates. In general, the formation of mixed micelles with other aliphatic acids causes a further drop in surface tension [17]. These alkyl chain intermediate products are further oxidized to give water-soluble substrates possessing a hydroxyl moiety. Thus the temporal variations observed in the surface tension behaviour during the photo-oxidative process reflect the decomposition of the hydrophobic alkyl chain and/or the hydrophilic moiety.

Plots of the CO_2 mineralization yield vs. the irradiation time for the three classes of surfactants are given in Figs. 2(a)–2(c). The photodegradation of the surfactants is so complicated that various photo-oxidative intermediates are generated. It is interesting to reveal the relationship between the structure of the surfactants and the photodegraded products before the formation of NH_4^+ and NO_3^- ions and CO_2 evolution. Although the experimental data shown in Figs. 2 and 3 do not fit elementary curves, the rate constants of initial generation of NH_4^+ and NO_3^- and CO_2 evolution up to an irradiation time of 2 h were calculated using pseudo-first-order kinetics in order to allow a quantitative comparison between the various systems. These rate constants are listed in Table 1.

The rate of CO_2 evolution for the cationic DPC and BTDAC species (Fig. 2(a)) is slower (9.3×10^{-4} min^{-1}) by a factor of approximately 2.4 to 4.5 than the rates observed (4.2×10^{-3} to 2.3×10^{-3} min^{-1}) for the non-ionic and amphoteric structures. For the last two classes of surfactants, the maximum yield (approximately 45%–55%) of carbon dioxide was noted after approximately 3–5 h of illumination; the cationic systems exhibit a continual increase in yield even after 9 h of irradiation.

The temporal evolution of ammonium and nitrate ions from the photo-oxidative destruction of the various surfactant systems is illustrated in Figs. 3(a)–3(c). The quantity of ammonium ions formed is larger than that observed for nitrate ions. The concentrations of NO_3^- remain constant at about 0.01 mM after about 8 h of irradiation irrespective of the surfactant structure. By contrast, the temporal profiles of the concentration of ammonium ions depend on the structure of the nitro-

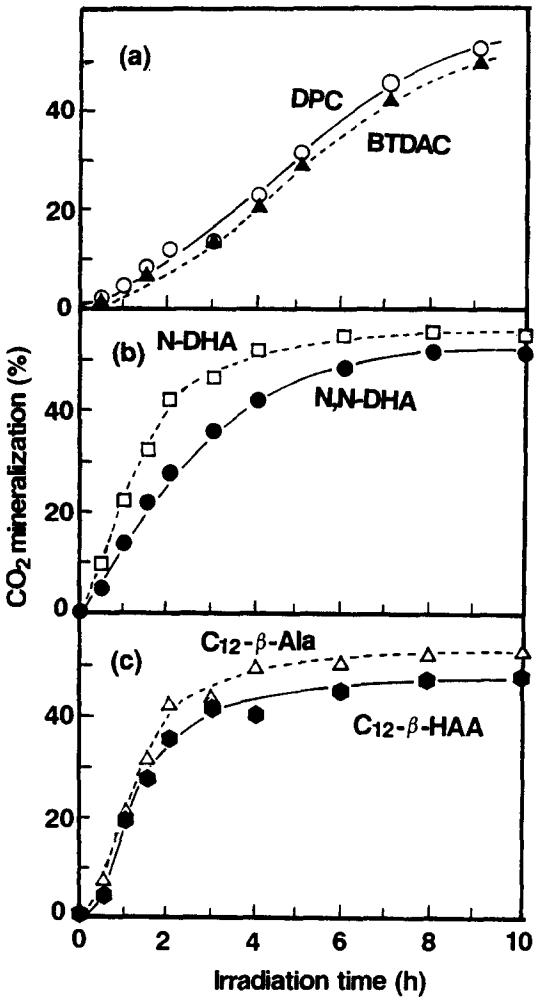

Fig. 2. Relationship between the CO_2 mineralization yield and the illumination time for (a) cationic surfactants: ○, DPC; ▲, BTDAC; (b) non-ionic surfactants: □, N-DHA; ●, N,N-DHA; (c) amphoteric surfactants: △, C_{12}-β-Ala; ●, C_{12}-β-HAA.

Table 1
Rate constants during the photo-oxidation of various surfactants

Surfactant	$k^{(1)}$ (min^{-1})		
	CO_2	NH_4^+	NO_3^-
Cationic			
DPC	9.3×10^{-4}	5.2×10^{-3}	4.8×10^{-4}
BTDAC	9.3×10^{-4}	1.4×10^{-3}	2.4×10^{-4}
Non-ionic			
N-DHA	4.2×10^{-3}	1.8×10^{-3}	2.4×10^{-4}
N,N-DHA	2.3×10^{-3}	1.5×10^{-3}	2.4×10^{-4}
Amphoteric			
C_{12}-β-Ala	4.0×10^{-3}	1.2×10^{-3}	4.2×10^{-4}
C_{12}-β-HAA	3.3×10^{-3}	1.3×10^{-3}	4.2×10^{-4}

gen moiety. The generation of nitrate ions occurs concomitantly with the formation of ammonium ions. The conversion of ammonium ions to nitrate ions is a slow process. (Under other conditions, about 10% of NH_4^+ was photoconverted to NO_3^- species after 6 h of illumination in aqueous TiO_2 dispersions [18].) Thus their formation from the mineralization of nitrogen-containing substrates presumably takes place by a different pathway. The concentration ratios, $[NH_4^+]/[NO_3^-]$, after 8 h of illumination are as follows: cationic DPC, 6.4; cationic BTDAC, 3.9; non-ionic N-DHA, 11.2; non-ionic N,N-DHA, 12.9; amphoteric C_{12}-β-HAA, 4.0; amphoteric C_{12}-β-Ala, 4.2. Data for the cationic surfactant BTDAC show an induction period in the formation of ammonium ions (Fig. 3(a)), contrary to DPC where no such induction period is seen. We presume that the formation of NH_4^+ occurs concurrently with the ring opening of the pyridinium moiety. In the BTDAC structure, the N atom is somewhat protected by the surrounding methyl, benzyl and dodecyl groups from reaching the catalytic site(s) on the TiO_2 particle surface; this may be responsible for the time lag in the formation of NH_4^+ ions. The tertiary amine in N,N-DHA produces a larger quantity of ammonium ions than the secondary amine in N-DHA, even though the formation occurs at nearly equal rates. Amphoteric surfactants produce

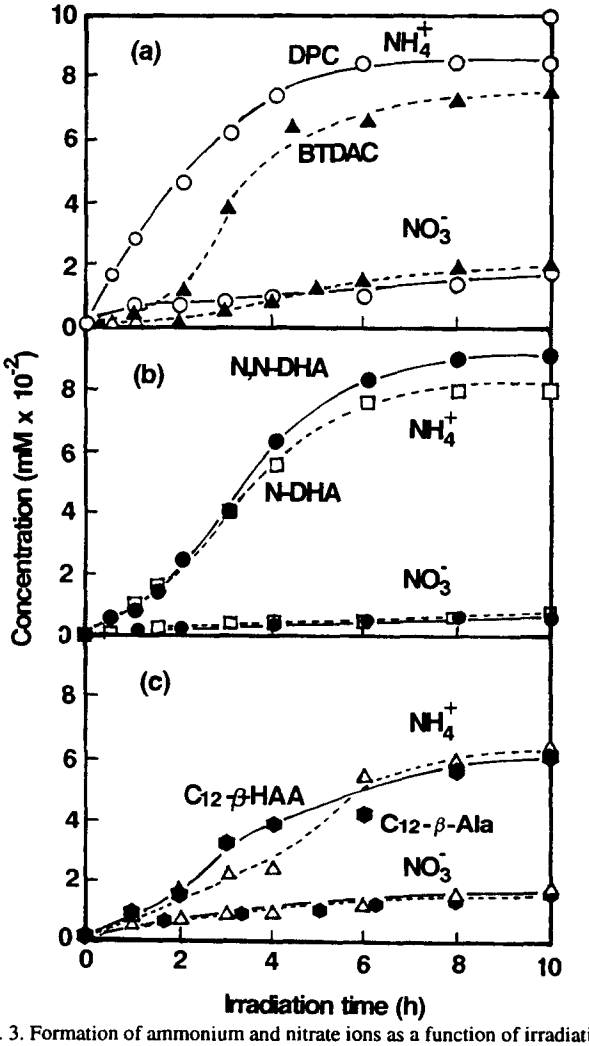

Fig. 3. Formation of ammonium and nitrate ions as a function of irradiation time in the photomineralization of (a) cationic surfactants: ○, DPC; ▲, BTDAC; (b) non-ionic surfactants: □, N-DHA; ●, N,N-DHA; (c) amphoteric surfactants: △, C_{12}-β-Ala; ●, C_{12}-β-HAA. Concentration, 1 mM.

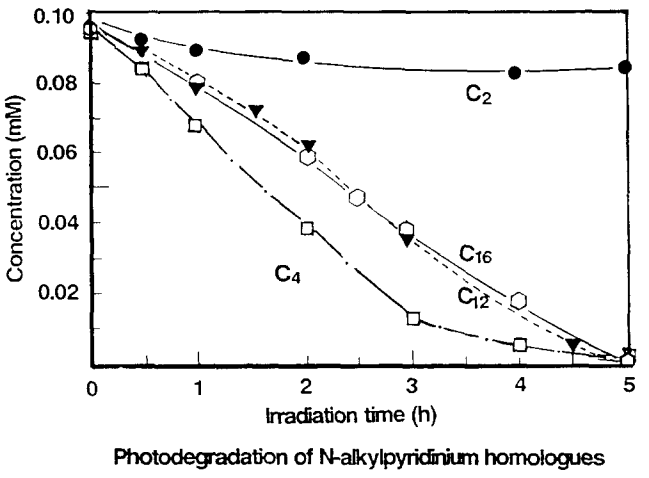

Fig. 4. Photocatalysed disappearance of the pyridinium ring in *N*-alkylpyridinium halides (●, C_2; □, C_4; ▼, C_{12}; ○, C_{16}) in the presence of TiO_2 (100 mg) on UV illumination with a mercury lamp.

smaller quantities of NH_4^+ and NO_3^- species than non-ionic and cationic surfactants. C_{12}-β-HAA exhibits a slightly faster formation of NH_4^+ ions than C_{12}-β-Ala. Finally, a comparison of the data in Figs. 2 and 3 shows that the formation of ammonium and nitrate ions occurs nearly concurrently with the evolution of carbon dioxide in the initial stages. The rate of NH_4^+ formation in the cationic surfactants is about 2.3 times faster than the rate of CO_2 evolution. However, in the non-ionic and amphoteric structures, the rate of NH_4^+ formation is 2–8 times slower than the rate of CO_2 evolution.

The effect of alkyl chain length (C_2, C_4, C_{12} and C_{16}) on pyridinium ring opening in the photo-oxidation of *N*-alkylpyridinium homologues in aqueous TiO_2 suspensions is illustrated in Fig. 4. The pyridinium rings with C_4, C_{12} and C_{16} alkyl chains are easily cleaved under the prevailing photocatalytic conditions. The rate of disappearance of the pyridinium ring, monitored by the changes in its 258 nm absorption band, follows first-order kinetics for the C_2 homologue (1.4×10^{-2} min^{-1}); by contrast, the rings in the C_{12} and C_{16} structures are converted via zero-order kinetics (about 3.3×10^{-4} min^{-1}, see Table 2).

Curiously, the pyridinium ring in the C_4 system disappears initially via zero-order kinetics (4.6×10^{-4} min^{-1}), and after about 3 h of irradiation, the kinetics change to first order (1.8×10^{-2} min^{-1}). We attribute this to a change in the length of the alkyl chain from C_4 to C_2 (note the near-identical rates). The behaviour of the ethylpyridinium bromide is peculiar: the ring absorption band persists even after 5 h of illumination, whereas the 258 nm absorption band has disappeared for the other homologues after this time. We infer that the extent of adsorption of ethylpyridinium bromide onto the TiO_2 particle surface is minimal, if not negligible. This further suggests that the alkyl group and the chain length are significant factors affecting the adsorption of surfactants onto solid surfaces.

Table 2
Rate constants for the disappearance of *N*-alkylpyridinium halides following photo-oxidation in irradiated aqueous TiO_2 dispersions

Alkyl group	$k^{(0)}$ (mM min^{-1})	$k^{(1)}$ (min^{-1})
Ethyl	–	1.4×10^{-2}
Butyl	4.6×10^{-4} [a]	1.8×10^{-2} [b]
Dodecyl	3.3×10^{-4}	–
Hexadecyl	3.3×10^{-4}	–

[a] Initially photo-oxidation occurs via zero-order kinetics.
[b] Subsequently, when the hydrocarbon chain length has shortened, photo-oxidation follows first-order kinetics.

3.2. NMR spectral profiles vs. irradiation time

The temporal NMR spectral patterns for the photo-oxidation of BTDAC and DPC solutions (1 mM; solvent D_2O) are illustrated in Figs. 5(a) and 5(b). For the BTDAC system, the resonance signals of the terminal methyl group (0.75 ppm) and the ethylene groups (1.17–1.45 ppm) in the long alkyl chain are broadened as oxidation proceeds to 9 h of illumination, after which the signals decrease in intensity. After 17 h of irradiation, these signals disappear. For DPC solutions, the same tendency is observed (see Fig. 5(b)). The benzyl proton signal at about 7.40 ppm also decreases with an increase in irradiation time. Similar observations are evident for the three NMR signals at 8.71, 8.40 and 7.92 ppm attributable to the pyridinium ring protons; the signals decrease in intensity with further irradiation. The common signal at 2.40 ppm for both BTDAC and DPC structures, generated on illumination, is assigned to the α-methyl proton of the alkyl amine formed. The signal for acetic acid at 1.90 ppm, which also develops during illumination, is observed in both BTDAC and DPC NMR spectral patterns. Also evident in Figs. 5(a) and 5(b) is the more rapid photo-oxidation of the pyridinium and benzyl groups compared with the alkyl chain which forms intermediates such as alkyl amines. The larger width of the alkyl chain proton signals infers that some of the alkyl moieties aggregate in the photo-oxidized intermediates to form rigid molecular assemblies.

Fig. 6 depicts the time course of the NMR spectral profile changes during the photo-oxidation of N,N-DHA solutions (1 mM; solvent D_2O). During the initial stage of illumination, a new resonance signal appears at 8.04 ppm; its intensity increases with illumination time. This low-field NMR signal is attributed to the formation of formaldehyde. The signals around 3.58 ppm of the hydroxyethyl moieties gradually decrease and new resonance signals are generated in the 3.0–3.7 ppm range for various oxidized intermediates. The three peaks at 0.76, 1.17 and 1.46 ppm, arising from the alkyl chain protons, also decrease in intensity within 1 h of irradiation as noted in the BTDAC and DPC NMR spectral profiles (Figs. 5(a) and 5(b)). These signals decrease up to 4 h of illumination when they disappear almost completely, and subsequently reappear after further irradiation (see the NMR spectral profile after 6 h of irradiation).

This disappearance/reappearance of NMR signals suggests that, during the photo-oxidative process, water-insolu-

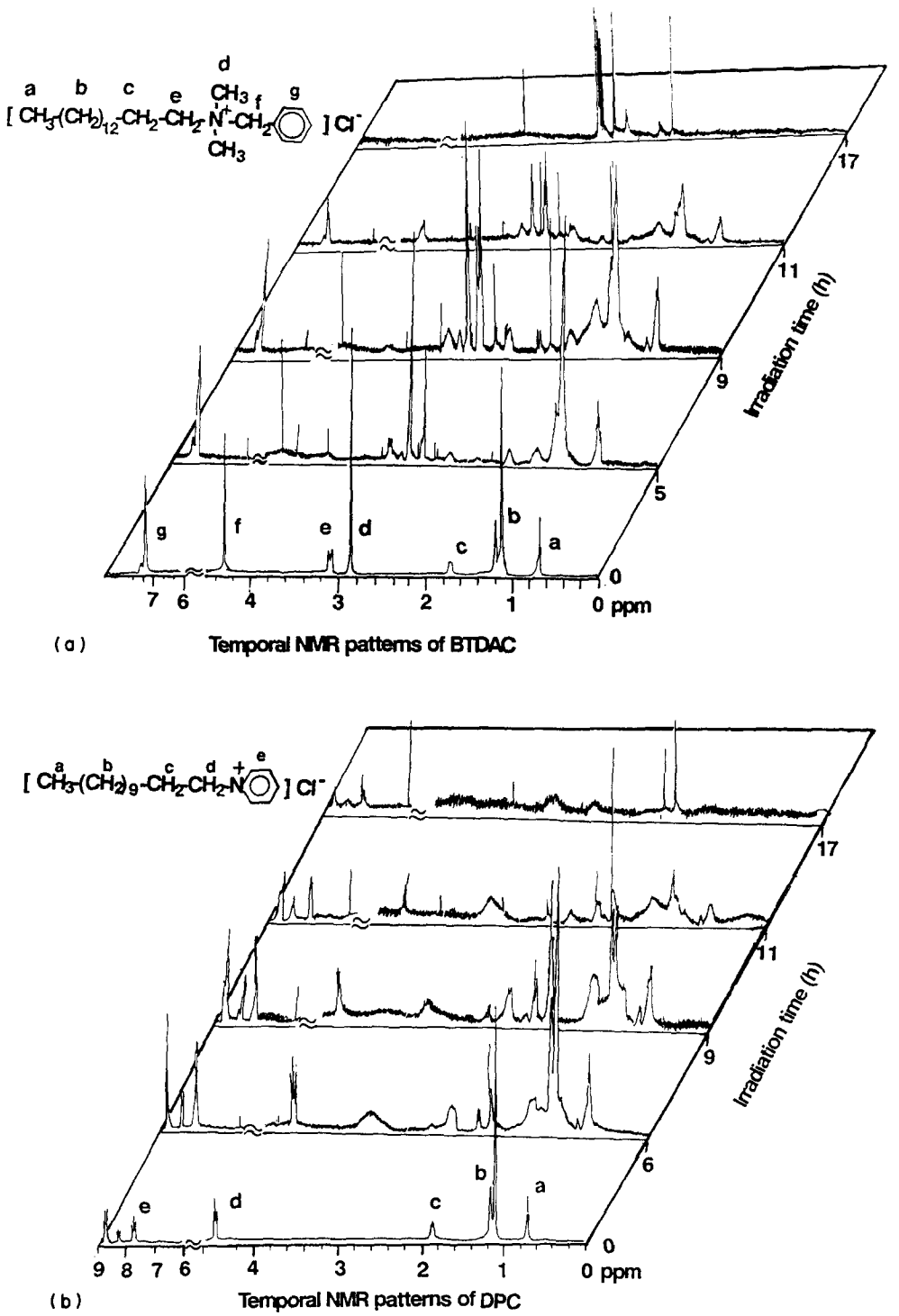

Fig. 5. Temporal NMR spectral profiles during the photo-oxidative degradation of (a) cationic BTDAC surfactant in D_2O solution (1 mM) and (b) cationic DPC surfactant in D_2O solution (1 mM).

ble intermediates are formed which possess a non-destructible alkyl chain but lack the hydrophilic hydroxyethyl moieties. These D_2O-insoluble intermediates could not be identified from the NMR spectra. Such behaviour was observed in 10 mM solutions of N,N-DHA but not at concentrations of 1 mM. Subsequent photo-oxidation of these unknown intermediates renders them soluble again in D_2O, and consequently their NMR signals reappear at 6 h of irradiation. This phenomenon correlates with the increase/decrease/increase behaviour noted in the surface tension measurements monitored during photo-oxidation (Figs. 1(a)–1(c)). The transverse relaxation time T_2 closely expresses the dependence (in part) of the linewidth of an NMR signal on dynamic molecular diffusion [19]. For exam-

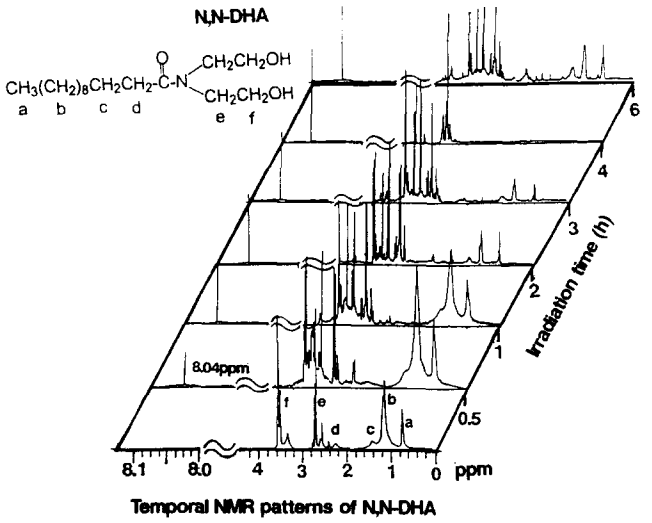

Fig. 6. Temporal NMR spectral profiles during the photo-oxidative decomposition of non-ionic N,N-DHA surfactant in D_2O solution (10 mM).

ple, extensive dynamic molecular movements result in long T_2 relaxation times, whereas slow molecular movements lead to short T_2 relaxation times. According to the equation

$$\delta\nu_{1/2}(\mathrm{Hz}) = 1/\pi T_2$$

the values of T_2 for the alkyl chain NMR signals are 8.2, 6.3 and 5.5 ms at 0, 0.5 and 1 h illumination times respectively ($\delta\nu_{1/2}$ is the linewidth of the alkyl chain signals at half-maximum amplitude). The T_2 relaxation time decreases with increasing irradiation time. This suggests that micellar aggregation behaviour in the photo- oxidized solution restricts the motion of intermediates with long alkyl chains. This phenomenon confirms that surface-active intermediates are produced during photomineralization. This inference is in keeping with the results noted in Fig. 1.

3.3. Proposed pathways for the photodegradation of the alkyl chain

Since the nitrogen-containing surfactants examined here possess a hydrophobic alkyl chain, both their adsorption onto the TiO_2 surface and their water solubility are affected by this alkyl chain and by the chain length. Photo-oxidation of alkyl groups is somewhat slower than oxidation of ionic and ethoxyl moieties [8b]. Details of the photo-oxidative pathway for these alkyl chains are not readily available. To gain insight into the mechanistic route(s) of alkyl chain photo-oxidation, we have examined the temporal variations in the NMR spectral profiles for the photo-oxidation of a 10 mM D_2O solution of sodium dodecanoate. The signal at 1.18 ppm, which is attributable to the alkyl chains, decreases with increasing illumination as shown in Fig. 7.

However, the 1.14 and 2.06 ppm signals for the terminal methyl protons and α-methylene protons respectively remain after 10 h of irradiation. The new signals (1.90 ppm, attributable to acetic acid) increase during photodegradation with

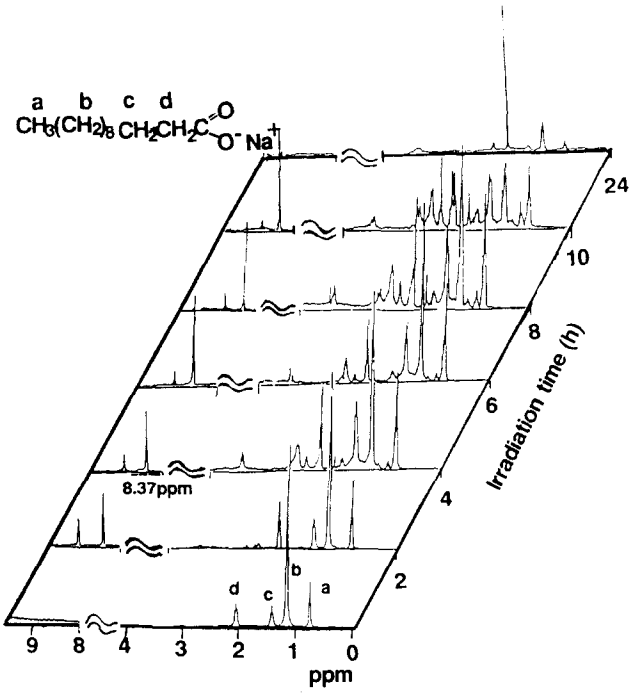

Fig. 7. Temporal NMR spectral profiles during the photo-oxidative decomposition of sodium dodecanoate in D_2O solution (10 mM).

the maximum value being reached after 24 h of irradiation. The low-field signal at 8.37 ppm, ascribed to the formyl derivative photointermediate, is initially observed and then disappears after 24 h of illumination. Results from the integration of the NMR peaks indicate that the starting structure having 12 carbon atoms is photo-oxidized to yield a structure with 11 carbons after 2 h of irradiation; this is then followed by a gradual decrease in the number of carbon atoms, one at a time, with the irradiation time. Following a somewhat longer illumination (about 10 h), an alkyl group containing four carbon atoms remains in solution. On further illumination to 24 h, the fate of the alkyl chain can no longer be monitored by NMR because of the interference from an ever increasing signal corresponding to that of acetic acid (1.99 ppm). These observations infer that the photo-oxidation of alkyl chains originates with sequential $^{\cdot}OH$ radical attack at the α-positions, one by one, and not at the ω-terminal carbon, as shown by the invariance of the peak intensity of the terminal methyl proton (1.44 ppm) even after long irradiation periods. The attack by the $^{\cdot}OH$ radical is the first step in the production of formic acid which ultimately is oxidized to CO_2. The continued photo-oxidative attack at the subsequent α-positions leads to fission of the C–C bonds yielding shorter chain lengths.

4. Conclusions

The rate of formation of ammonium ions is slower than that of CO_2 evolution for both amphoteric and non-ionic surfactants, but faster for cationic surfactants. The yield of

NH_4^+ ions is about 4–13 times larger than that of NO_3^- ions. The rate of production of NO_3^- ions is approximately the same for all the surfactant structures examined and the quantity of nitrate produced is also nearly the same (0.01 mM). The photoconversion of the nitrogen moiety occurs concomitantly with the photo-oxidation of the alkyl chain. The surface-active intermediates are produced in the initial stage of the photo-oxidative process. NMR spectral profiles show that alkyl chains are photo-oxidized at the α-carbons with scission of the C–C bond to shorten the chains. Adsorption onto the TiO_2 particulate surface is probably a rate-determining step in the photomineralization of surfactants since the hydrophobic alkyl moiety appears to play an important role.

Acknowledgments

Our work in Tokyo was supported by the Japan International Cooperation Agency (JICA) and the Cosmetology Research Foundation (Japan), in Torino by the CNR (Roma, Italy) and in Montréal by the NSERC (Canada). We are grateful to our coworkers for technical assistance and to Professor M. Grätzel (Lausanne, Switzerland) and Dr. P. Pichat (Lyon, France) for useful discussions.

References

[1] Y. Ichikawa, Y. Kitamatu and N. Hosoi, *J. Ferment. Technol., 56* (1978) 403.

[2] (a) S. Ono, A. Masuyama and M. Okahara, *J. Org. Chem., 55* (1990) 4461. (b) S. Yamamura, K. Shimaki, T. Nakajima, T. Takeda, I. Ikeda and M. Okahara, *J. Jpn. Oil Chem. Soc., 40* (1991) 16.

[3] (a) A. Kotronarou, G. Mills and M.R. Hoffmann, *J. Phys. Chem., 95* (1991) 3630. (b) N. Serpone, R. Terzian, P. Colarusso, C. Minero, E. Pelizzetti and H. Hidaka, *Res. Chem. Intermed., 18* (1992) 183.

[4] O. Legrini, E. Oliveros and A.M. Braun, *Chem. Rev., 93* (1993) 671.

[5] M.A. Fox and M.T. Dulay, *Chem. Rev., 93* (1993) 3141.

[6] G. Mills and M.R. Hoffmann, *Environ. Sci. Technol., 27* (1993) 1681.

[7] (a) H. Hidaka, K. Nohara, J. Zhao, N. Serpone and E. Pelizzetti, *J. Photochem. Photobiol. A: Chem., 64* (1992) 247. (b) H. Hidaka, T. Nakamura, A. Ishizaka, M. Tsuchiya and J. Zhao, *J. Photochem. Photobiol. A: Chem., 66* (1992) 367.

[8] (a) H. Hidaka, J. Zhao, E. Pelizzetti and N. Serpone, *J. Phys. Chem., 96* (1992) 2226. (b) H. Hidaka, J. Zhao, K. Kitamura, K. Nohara, N. Serpone and E. Pelizzetti, *J. Photochem. Photobiol. A: Chem., 64* (1992) 103. (c) J. Zhao, H. Hidaka, A. Takamura, E. Pelizzetti and N. Serpone, *Langmuir, 9* (1993) 1646.

[9] (a) C.K. Grätzel, M. Jirousek and M. Gratzel, *J. Mol. Catal., 39* (1987) 347. (b) H. Hidaka, J. Zhao, Y. Satoh, K. Nohara, E. Pelizzetti and N. Serpone, *J. Mol. Catal., 88* (1994) 239.

[10] H. Hidaka, K. Takashima, K. Nohara, J. Zhao, E. Pelizzetti and N. Serpone, *New J. Chem., 18* (1994) 541.

[11] (a) G.K.-C. Low, S.R. McEvoy and R.W. Matthews, *Environ. Sci. Technol., 25* (1991) 460. (b) G.K.-C. Low, S.R. McEvoy and R.W. Matthews, *Chemosphere, 19* (1989) 1611.

[12] (a) E. Pelizzetti, C. Minero, P. Piccinini and M. Vincenti, *Coord. Chem. Rev., 125* (1993) 183. (b) E. Pelizzetti, C. Minero, E. Pramauro, M. Barbeni, V. Maurino and M. Tosato, *Chim. Ind. (Milano), 69* (1987) 88.

[13] Degussa Canada Ltd., *Technical Bulletin No. 56*, Degussa Canada Ltd., Burlington, Ont., Canada, 1982.

[14] (a) D. Lawless, N. Serpone and D. Meisel, *J. Phys. Chem., 95* (1991) 5166. (b) N. Serpone, D. Lawless, R. Terzian and D. Meisel, in R. McKay and J. Texter (eds.), *Electrochemistry in Colloids and Dispersions*, VCH, New York, 1992, pp. 399–416. (c) O.I. Micic, Y. Zhang, K.R. Cromack, A.D. Trifunac and M.C. Thurnauer, *J. Phys. Chem., 97* (1993) 7277.

[15] (a) D. Bahnemann, J. Cunningham, M.A. Fox, E. Pelizzetti and N. Serpone, in D. Crosby, G. Helz and R. Zepp (eds.), *Aquatic and Surface Photochemistry*, Lewis, Boca Raton, FL, 1993, pp. 261–316. (b) M.A. Fox, in P. Mariano (ed.), *Advances in Electron Transfer Chemistry*, JAI Press, Greenwich, CT, 1991, pp. 1–53.

[16] (a) H. Hidaka, J. Zhao, K. Nohara, K. Kitamura, Y. Satoh, E. Pelizzetti and N. Serpone, in D.F. Ollis and H. Al-Ekabi (eds.), *Photocatalytic Purification and Treatment of Water and Air*, Elsevier, Amsterdam, 1993, pp. 251–260. (b) E. Pelizzetti, C. Minero, H. Hidaka and N. Serpone, in D.F. Ollis and H. Al-Ekabi (eds.), *Photocatalytic Purification and Treatment of Water and Air*, Elsevier, Amsterdam, 1993, pp. 261–274.

[17] H. Hidaka, S. Yoshizawa and M. Moriya, *J. Jpn. Oil Chem. Soc., 31* (1982) 489.

[18] E. Pelizzetti et al., unpublished observations, 1993.

[19] R.S. Drago, *Physical Methods in Chemistry*, Saunders, Philadelphia, 1977, pp. 203–206.